1661-8726/07/020281-12
DOI 10.1007/s00015-007-1218-0
Birkhäuser Verlag, Basel, 2007

Swiss j. geosci. 100 (2007) 281–292

Slip rates variability and sediment mobilization on a shallow landslide in the northern Swiss Alps

Marco Schwab[1], Christine Läderach[1], Dirk Rieke-Zapp[1] & Fritz Schlunegger[1]

Key words: sediment mobilization, slip rates, landslide, Central Switzerland, geomorphology

ABSTRACT

Geomorphic and morphometric data imply that process rates of the Schimbrig landslide, located in the Entle watershed (Central Switzerland), are still limited by the elevation of the LGM base level. At present, the Entle watershed is in a stage of adjusting to the lowered post-glacial base level as indicated by knick zones in the trunk stream. Some thousands of years later when these knick zones will reach the Schimbrig site, we anticipate a substantial increase in process rates and sediment flux for the landslide.

The pattern of slip rates was measured on the Schimbrig landslide over a 14-months period. We propose that a Bingham plastic model explains much of how measured slip rates are linked to the observed topography, climatic variations and thickness variability of the landslide mass. This model explains why slip rates have been highest where the thickness of the material is substantially higher. It also explains why slip rates are highest in late summer/autumn and early spring. It appears then that snow melt in spring and decreasing temperatures in late summer/autumn potentially result in a high retention of the pore water and thus in a low viscosity of the material, which, in turns, promotes slip rates. Interestingly, an extreme rainstorm like the one of August 2005 only had a local impact on the landslide mass by triggering small scale earth flows and debris flows. This implies that the earth slide material does not directly respond to an episodic pattern of rainfall. Such precipitation events, however, superimpose a smaller-scale imprint on the landslide relief.

1. Introduction

Hillslope instabilities and landslides in particular represent a substantial potential for risks in mountainous regions and are a dominant source of sediment in several mountain river basins (Korup 2004; 2005; Schürch et al. 2006). In the Swiss Alps, up to 30% are located on Flysch terrains, and 40% of them are considered to be unstable (Latelin et al. 1997). These instabilities occur at scales up to several hundreds of meters to kilometers and show variations in slip rates ranging from the millimeter- to the meter-scale per month. In this paper, the term 'activity' is used to describe a measurable movement, i.e. slip rates at the centimeter- to decimeter-scale per month. In 1994, a period of high activity was observed in several Flysch regions along the northern Voralps forming landslides particularly in the western foothills of the Swiss Alps (Liniger & Kaufmann, 1994a, b). For instance, Falli Hölli (Canton Fribourg) (Caron et al. 1996) and Hohberg (Canton Fribourg) (Raetzo et al. 2000), being the most prominent ones among them, caused substantial damages to infrastructure and have limited landuse until today. Such landslides, however, have not been continuously surveyed. In particular, when the landslide activity and hence the risk for damages decreases, surveys are terminated. Consequently, there is only limited quantitative information about low-activity periods of Flysch landslides in Switzerland. Therefore, the knowledge of the variability in slip rates and the spatial extension of landslides is limited and commonly covers only the high-activity-stage in a landslide's development. Similarly, there are only few survey-based studies that aim at interpreting the mechanical properties and the architecture of landslides (e.g., Coe et al. 2003; Schürch et al. 2006).

An example of such hillslope instability on a Flysch terrain is the Schimbrig landslide in the Entlen watershed, southwest of Lucerne, Central Switzerland (Fig. 1). It is a long-known landslide that has experienced multiple reactivation events until today. The last prominent one occurred in 1994 after periods of enhanced precipitation rates and wet autumns (Liniger & Kaufmann 1994a). The 1994 event was a thread to infrastructure, and consequently, it was monitored to detect the development of slip rates. After 1995, the activity of the landslide decreased and only few measurements of slip rates were done during the succeeding three years.

Institut für Geologie, Universität Bern, Baltzerstrasse 1+3, 3012 Bern, Switzerland. E-mail: schwab@geo.unibe.ch

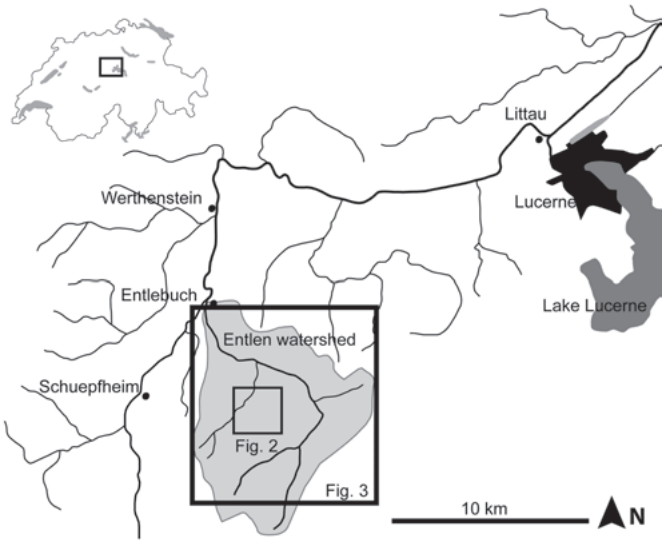

Fig. 1. Geographical overview of the study area. The boxes show the spatial extents of Figure 2 and 3.

The objective of this paper is to present the slip rates of the Schimbrig landslide that were measured during one year, and correlate these data to topographic and climatic boundary conditions. The ultimate goal is to detect the most important controls on the dynamics of the Schimbrig landslide and to propose a mechanical model that allows explaining and integrating climate and thickness variability. Note that we do not aim at delivering predictive tools for landslide activity in general and for the Schimbrig landslide in particular. We rather intend to identify a conceptual model of earth slide activity that predicts from a generic point of view how these slides potentially respond to changes in boundary conditions. In this paper we will use the nomenclature of Cruden and Varnes (1996) to describe landforms and processes, and we will use the term "Schimbrig landslide" when it refers to its geographic extent.

2. Settings

2.1 Geological Setting

The Schimbrig landslide is located at the northern foothills of the Central Alps in Switzerland (Lucerne area). In this area, the Alpine Border Chain is made up of the Wildhorn nappe that forms the steep walls of siliceous limestones (Helvetischer Kieselkalk). The Wildhorn nappes overlay the marl-rich Subalpine Flysch (Bieri 1982) that was deposited in a turbiditic environment between the Upper Cretaceous and the Eocene during Alpine orogenesis and that was then incorporated into the Alpine orogenic wedge subsequent to deposition (Pfiffner 1986). At present, the Subalpine Flysch lies on top of the Subalpine Molasse with a thrust plane between them (Fig. 2).

The units of the Subalpine Molasse date from Early Oligocene to Late Miocene (Matter 1964; Gasser 1966; Gasser 1968; Schlunegger et al. 1996). They are composed of four main units, from which only the Rupelian Lower Marine Molasse (UMM) and the Chattian Lower Freshwater Molasse (USM) are present in the study area. They represent a succession from deep marine to terrestrial deposits. These deposits were then incorporated in the orogenic wedge in the Early Miocene (Schlunegger et al. 1997; Schlunegger et al. 1998; Kempf & Pfiffner 2004).

During the Pleistocene, the landslide area was covered by ice sheets during glacial time intervals. After the retreat of the glacial ice sheet at the end of the last glacial maximum (LGM) at approximately 15 ka, a meter-thick layer of unconsolidated

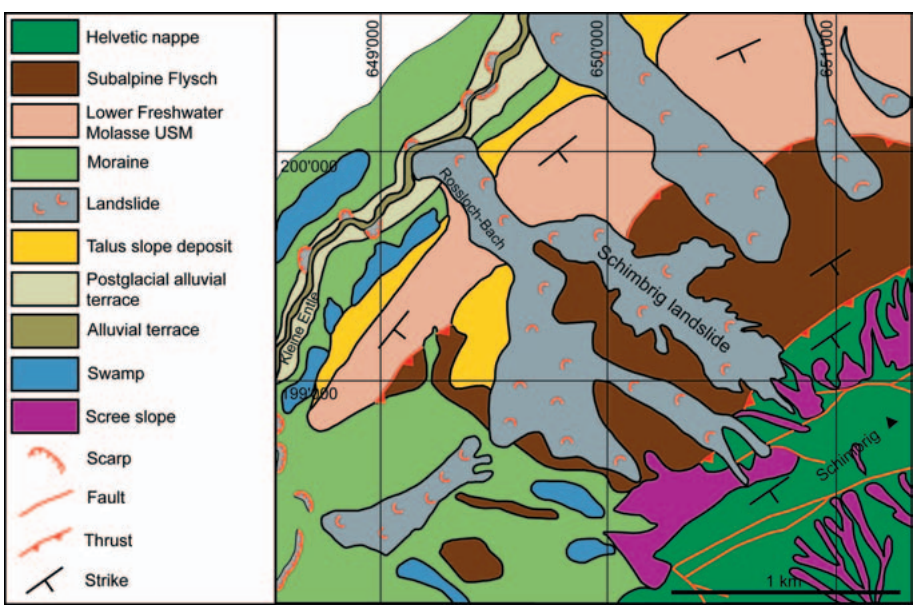

Fig. 2. Geological overview of the Rossloch-Bach watershed (modified after Mollet, 1921). Coordinate system CH1903LV03.

ground moraine remained at the foothills of mount Schimbrig. These till deposits have promoted hillslope instabilities and have represented the most important sediment sources for landslides (Mollet 1921).

2.2 Geomorphological setting

The drainage basin, in which the Schimbrig landslide is located, is drained by two major trunk streams: Grosse and Kleine Entle (Fig. 3). The Grosse Entle has its source in the first intra-alpine valley SE of the Helvetic Border Chain. It transects this chain in a narrow passage east of mount Schimbrig. The Kleine Entle drains the segment north of this chain and discharges into the Grosse Entle northwest of mount Schimbrig.

The Schimbrig landslide is located within the approximately 4 km^2-large catchment of the Rossloch-Bach in the Kleine Entle drainage basin (Fig. 3). The headwaters of the Rossloch-Bach comprise the hillslopes that are underlain by Subalpine Flysch deposits and Pleistocene glacial till. These rock types have a low mechanical strength and thus promote hillslope instabilities. Before debouching into the Kleine Entle, the Rossloch-Bach transects a ridge made up of the conglomerate-mudstone alternation of the Lower Freshwater Molasse (Fig. 2).

The Schimbrig landslide has a long history with cycles of reactivations and changing slip rates. Those cycles have resulted in the shape of the modern morphology of the Rossloch-Bach watershed. The presence of a landslide in the watershed was already identified in 1921 by Mollet. The landowners and farmers in this region have been aware of the difficulty of land use, and they have known of several incidents of slide events. As mentioned above, a prominent earth slide event occurred in spring 1994 (Liniger & Kaufmann 1994a), when farmers observed damages on one road in the upper portion of the landslide. At the end of summer 1994 there was an exponential increase in process rates at the landslide's toe (Liniger & Kaufmann 1994a). An access road as well as some buildings and culverts were destroyed, and the course of the Rossloch-Bach was redirected due to the closure of the initial channel.

In mid August 2005, a high-magnitude, four days-long precipitation event releasing approximately 130 mm of rain triggered several decameter-scale earth flows and debris flows on the Schimbrig earth slide surface. The access road on the uppermost part of the landslide was destroyed at several locations; the biggest incident triggered multiple debris flows which deepened the channel of the Rossloch-Bach by 1 m along the entire landslide.

2.3 Climate and hydrology

To concatenate process rates of the earth slide with climatic influences we examined datasets of precipitation rates and water runoff of the receiving trunk stream (Waldemme) during the last 20 years (Fig. 4). The data was recorded at stations of the Federal Office of Meteorology and Climatology (MeteoSwiss) and of the Federal Office for the Environment (FOEN).

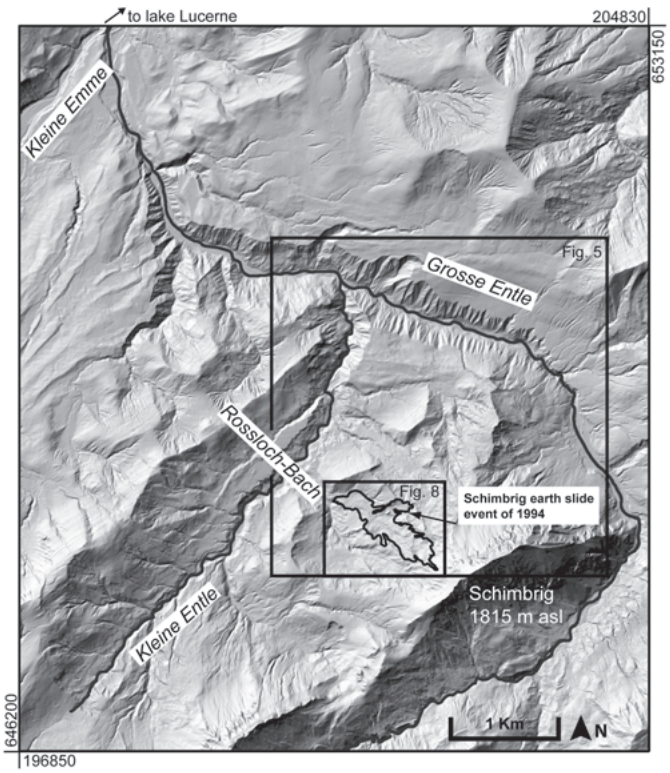

Fig. 3. Overview over the Entle watershed with the extent of the Schimbrig earth slide event of 1994. The extent of Figures 5 and 8 are marked. Data © GIS Kanton Luzern. Coordinate system CH1903LV03.

Precipitation was measured daily in Entlebuch; water runoff of the Kleine Emme was recorded daily at Werthenstein and suspended sediment concentration (SSC) at Littau (see Fig 1 for locations of the stations). The comparison of the climatic records from 1984 until 2005 displays a good correlation between the precipitation and the runoff data (Fig. 4). The precipitation and the runoff curve show a seasonal trend with maximum magnitudes in late summer (S) and minimal values in winter (W). Similarly, sediment load concentrations reach highest magnitudes in late summer and increase immediately after the peaks of precipitation and runoff (see below).

3. Methods

In order to yield a detailed knowledge of the seasonal and spatial variability in the earth slide's slip rates, we measured the movements of the Schimbrig landslide during one year between 26th October 2004 and 15th November 2005. This was done using a differential GPS. Field mapping, supported by high resolution digital elevation model data, yielded information about the geomorphic properties (extensive or compressive features) of the landslide. This information were then interpreted in the context of the boundary conditions defined by climate and topography and the earth slide's architecture.

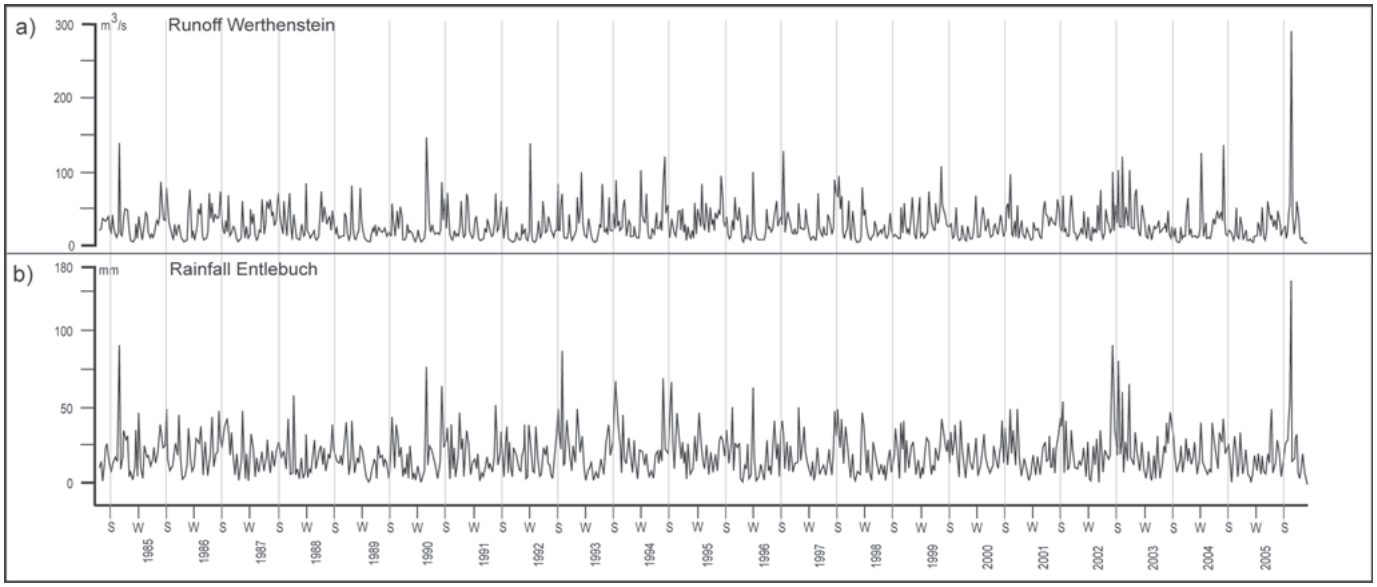

Fig. 4. Plot of (a) runoff and (b) precipitation rates from 1984 until 2005. The climatic datasets are taken from the Federal Office of Meteorology and Climatology (MeteoSwiss) and Federal Office for the Environment (FOEN). Location of the gauges are presented on Figure 1.

3.1 Installation of points

The first measurements of the earth slide's slip rates included the geodetic survey of 20 points in 1994, 1995 and some in 1998 (Liniger et al. 1994b). The survey of points located on the lowermost part of the earth slide yielded average slip rates of 1 m up to 3 m per month between 1994 and 1998 (Schnyder, pers. comm. 2004). After 1998, the slip rates decreased to the centimeter-scale per month. The cumulative displacement from 1994 to 2004 is on the range of 150 m based on 11 points (out of the 20 originally). In addition, 40 new points were installed to yield a complete survey. Seven points were installed outside of the earth slide limit as control points, six points were lost during the survey and twenty six were successfully measured seven times between September 2004 and November 2005. The points are oriented in several lines that run across the whole earth slide (Fig. 8b). These lines cover the three main zones of the earth slide including the toe with evidence for sediment accumulation, the central part and the head where the slopes are steepest. In-between these lines, the dense conifer vegetation does not allow taking any accurate GPS measurements. The points were placed in a wide variety of topographic features (scarps, hollows and suspicious breaks in the topography) to detect the sliding rates in different geomorphic environments (see Fig. 8b for the exact location of the points and Table 1 for measurements).

For the measurements, a nail stamped on a 40 cm high dowel with a cavity on its head was used. These cavities marked the position that was then iteratively measured.

3.2 Survey with a differential GPS (DGPS)

For the high-resolution survey we used two methods of differential GPS (DGPS) setups. The one used in all but the last session was Real-Time-Kinematic (RTK) survey done with the DGPS System 500 of Leica. It uses an arrangement of two GPS receivers, one served as a static reference placed in a stable position with known XYZ-coordinates (base station). The other receiver was the mobile rover that was then used to measure the survey points. The reference station constantly measured its positions; these measurements were then compared with its real position, and the calculated differences were sent as correction signal per radio to the mobile rover. This latter station corrected the measured position accordingly to get accurate position sensing. However, in order to relate these differences to the national coordinate system, a triangulation point with the exact coordinates had to be considered for the survey.

For the last session, we used a Post-Processing survey with DGPS. In this case, the measurements were taken only with the mobile rover of Leica GPS System 500. The correction information was then obtained from the Federal Office of Topography (Swisstopo) to minimize errors.

3.3 Calculation of slip rates on the earth slide

The information recorded during the GPS survey was: coordinates in northing, easting and ellipsoidal height in the local coordinate system of Switzerland (CH1903), date and time, error for northing, easting and ellipsoidal height and, calculated from the errors, the coordinate quality in the 3-dimensional space.

To acquire the slip rates between two surveys, the following calculations were used:

Table 1. Coordinates of the initial points followed by the displacement between each survey (all units in m). Also presented is the quality of the measurements and the total cumulative displacement and orientation. Shaded measurements are below the threshold quality.

	28-Sep-04				26-Oct-04		22-Nov-04		1-May-05		22-Jun-05		13-Aug-05		15-Nov-05		total displacement		
Point	N	E	H (ellipsoid)	cqual	mvec t0 t1	cqual	mvec t1 t2	cqual	mvec t2 t3	cqual	mvec t3 t4	cqual	mvec t4 t5	cqual	mvec t5 t6	cqual	mvec t0 t6	azm t0t6	cqual
L01	649752.54	199608.07	1103.51	0.0155	0.22	0.0252	0.09	0.0132	0.81	0.0175	0.13	0.0158	0.19	0.0176	0.49	0.0018	1.85	285.3	0.1066
L02	649744.17	199619.61	1099.21	0.0156	0.17	0.0254	0.09	0.0129	0.85	0.0152	0.12	0.0153	0.23	0.0166	0.46	0.0021	1.86	276.0	0.1031
L03	649733.88	199629.69	1095.40	0.0165	0.18	0.0253	0.09	0.0132	0.75	0.0176	0.12	0.0208	0.18	0.0249	0.45	0.0011	1.69	257.8	0.1194
L04	649744.20	199648.77	1100.56	0.0135	0.09	0.0285	0.09	0.0216	0.40	0.0173	0.06	0.0194	0.14	0.0207	0.18	0.0014	0.85	225.3	0.1224
L11	649774.35	199578.52	1111.38	0.0151	0.08	0.0291	0.04	0.0182	0.04	0.0151	0.04	0.0203	0.02	0.0213	0.10	0.0023	0.07	26.0	0.1214
L12	649773.95	199588.61	1112.05	0.0129	0.19	0.0267	0.02	0.0155	0.03	0.0164	0.02	0.0134	0.01	0.0192	0.16	0.0016	0.08	13.3	0.1057
L13	649780.20	199641.64	1109.63	0.0147	0.14	0.0265	0.04	0.0135	0.02	0.0153	0.01	0.0159	0.02	0.0130	0.15	0.0009	0.06	89.1	0.0998
L31	650141.77	199351.71	1202.12	0.0295	0.05	0.0145	0.02	0.0172	0.04	0.0139	0.01	0.0214	0.02	0.0132	0.14	0.0006	0.14	5.6	0.1103
L32	650098.20	199428.89	1186.08	0.0170	0.02	0.0128	0.01	0.0192	0.03	0.0134	0.02	0.0134	0.02	0.0195	0.13	0.0007	0.14	23.4	0.0960
L33	650143.73	199440.54	1189.78	0.0153	0.04	0.0163	0.02	0.0157	0.07	0.0151	0.01	0.0194	0.01	0.0132	0.17	0.0004	0.27	285.4	0.0954
L34	650179.34	199420.21	1195.18	0.0203	0.05	0.0178	0.04	0.0158	0.11	0.0170	0.03	0.0182	0.05	0.0157	0.15	0.0005	0.36	307.3	0.1053
L36	650192.77	199462.95	1196.54	0.0130	0.11	0.0196	0.06	0.0160	0.12	0.0197	0.03	0.0228	0.05	0.0277	0.23	0.0005	0.46	254.8	0.1193
L41	650258.65	199405.03	1212.71	0.0462	0.43	0.0246	0.28	0.0120	1.30	0.0137	0.30	0.0150	0.53	0.0233	1.78	0.0005	4.60	338.9	0.1353
L42	650305.18	199459.88	1219.58	0.0171	0.08	0.0182	0.02	0.0142	0.01	0.0181	0.01	0.0204	0.03	0.0249	0.14	0.0011	0.08	29.5	0.1140
L43	650310.06	199485.16	1219.90	0.0327	0.11	0.0215	0.02	0.0233	0.08	0.0119	0.01	0.0202	0.03	0.0361	0.17	0.0007	0.26	370.8	0.1464
L44	650341.49	199530.87	1224.31	0.0263	0.06	0.0142	0.02	0.0159	0.04	0.0187	0.04	0.0140	0.03	0.0235	0.08	0.0006	0.15	239.8	0.1132
L45	650341.21	199607.34	1246.67	0.0282	0.03	0.0175	0.04	0.0182	0.02	0.0166	0.02	0.0295	0.02	0.0299	0.14	0.0008	0.14	27.4	0.1407
L46	650256.83	199385.30	1217.65	0.0410	0.26	0.0167	0.17	0.0144	0.86	0.0171	0.16	0.0175	0.28	0.0188	1.01	0.0006	2.73	324.6	0.1261
L51	650544.80	199054.65	1367.06	0.0166	0.03	0.0195	0.02	0.0140	0.01	0.0157	0.01	0.0153	0.02	0.0154	0.16	0.0005	0.16	26.6	0.0970
L52	650598.42	199033.20	1364.26	0.0174	0.02	0.0223	0.02	0.0198	0.03	0.0161	0.04	0.0161	0.01	0.0315	0.22	0.0007	0.24	1.1	0.1239
L5D	650554.08	199115.79	1343.39	0.0230	0.03	0.0196	0.04	0.0182	0.02	0.0210	0.02	0.0167	0.02	0.0220	0.19	0.0009	0.20	339.0	0.1214
L5C	650605.65	199082.53	1354.05	0.0123	0.02	0.0220	0.01	0.0141	0.02	0.0172	0.02	0.0139	0.03	0.0140	0.18	0.0007	0.19	345.0	0.0942
L5B	650649.92	199115.11	1363.07	0.0159	0.02	0.0186	0.01	0.0156	0.01	0.0197	0.01	0.0152	0.01	0.0194	0.15	0.0016	0.14	339.8	0.1060
L53	650660.06	199164.77	1363.38	0.0727	0.11	0.0169	0.04	0.0332	0.02	0.0169	0.02	0.0128	0.02	0.0205	0.16	0.0010	0.06	380.2	0.1740
L54	650692.69	199194.04	1378.18	0.0451	0.04	0.0165	0.02	0.0165	0.03	0.0275	0.04	0.0162	0.03	0.0159	0.18	0.0008	0.13	355.9	0.1385
L65	650638.23	198972.78	1412.08	0.0201	0.03	0.0152	0.00	0.0223	0.01	0.0218	0.02	0.0176	0.02	0.0230	0.95	0.0749	0.95	32.6	0.1949
L69	650752.44	199076.77	1409.71	0.0193	0.03	0.0143	0.01	0.0162	0.05	0.0190	0.10	0.0165	0.02	0.0174	0.37	0.0250	0.36	218.7	0.1277

Movements (main vector, *mvec*) between one survey (t_1) and the next (t_2):

$$mvec = \sqrt{(\Delta N^2 + \Delta E^2 + \Delta H^2)} \quad (1)$$

where $\Delta N = N(t_2) - N(t_1)$ is the difference in the northing coordinate. *E* (easting) and *H* (ellipsoidal height) are treated in an analogous way.

Movements per month (main vector monthly, $mvec_{mon}$):

$$mvec_{mon} = \left[\frac{mvec}{\Delta d}\right] \times 30 \quad (2)$$

where Δd are the days which passed between t_1 and t_2.

$$azm = \arctan = \left[\frac{\Delta E}{\Delta N}\right] \quad (3)$$

where *azm* (azimuth) is the direction of the movement in a 360° horizontal circle.

As a verification of the measured positions the calculated main vectors have been compared with the coordinate quality *(cqual)*. Displacements smaller than the quality value are highlighted in Table 1.

3.4 GIS analysis, mapping

The visualization of the process rates and directions was performed in ESRI ArcGIS v9. We used ArcMap and ArcScene to display and to analys the slip rates in comparison with topographic features extracted from the geomorphologic map. The base for this analysis was the Digital Elevation Model (DEM) with a resolution of 2 m × 2 m (GIS Kanton Luzern 2006) and the topographic map of the region at the scale of 1:10'000 (GIS Kanton Luzern 2006). In order to interpret the process rates in a geomorphic context, we mapped the earth slide area and the different topographic domains at a scale of 1:10'000. This information was added into the ArcGIS database to be analysed with the survey results. Mapping was performed in early August 2005. Therefore, the numerous small scale scarps and the channel widening related to the severe storm event in mid August 2005 do not appear on the map. Morphometric calculations were performed on the 2 m resolution DEM using standard GIS tools.

4. Results

4.1 Morphology of Entle watershed

The Entle River defines the base level for the Schimbrig landslide and thus exerts a potential control on the process rates of the earth slide. In particular, enduring incision of the Entlen river might enhance surface erosion and slip rates. Therefore, the morphology of the Entle watershed is considered in more detail here based on field observations and analyses of morphometric properties.

After the deglaciation which caused the base level to lower by approximately 150 m (Schlunegger & Hinderer 2003), the drainages surrounding the Entle catchment adjusted their longitudinal stream profiles by incision and headward erosion (e.g., Schlunegger & Schneider 2005, for a similar situation farther north), forming canyons that are approximately 6 km long, 600 m wide and 150 m deep. The longitudinal stream profiles extracted from the DEM, show well defined knick zones for both the Kleine and Grosse Entle (Fig. 5). The slope plot for the region, also extracted from the DEM, illustrates that beneath the knick zones, the hillslopes bordering the canyons are up to 30° steep (Fig. 5). At the lower termination of the

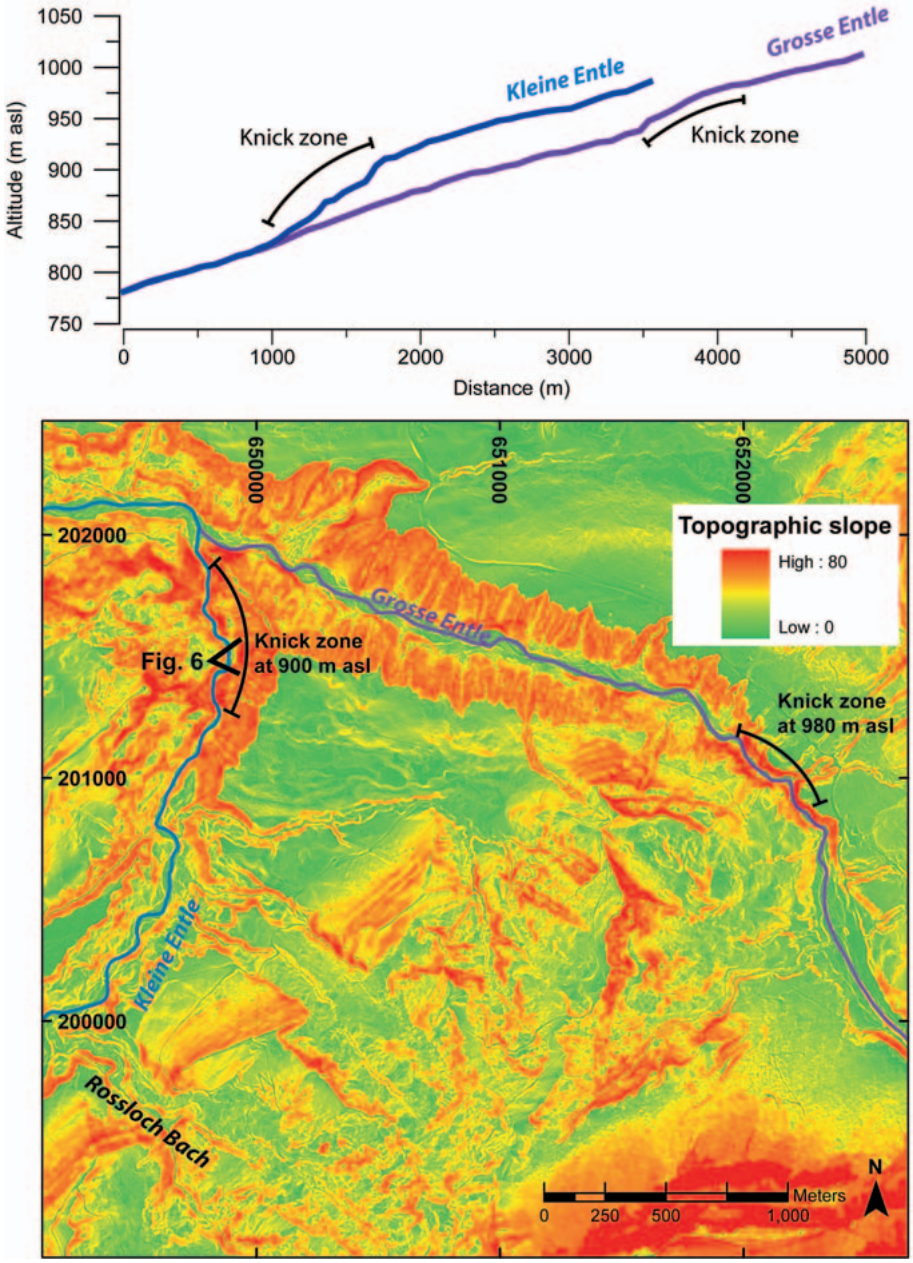

Fig. 5. Longitudinal stream profiles of the Kleine Entle (blue) and of the Grosse Entle (purple), and pattern of slope angles (topographic slope in degrees) of the area in which the knick zones are located. Data© GIS Kanton Luzern.

knick zones, the channel floors expose the bedrock that is a conglomerate-sandstone-alteration of the USM in the Grosse Entle, and sandstones and mudstones of the UMM in the Kleine Entle. There, the hillslopes bordering the channels are up to 50° steep and show multiple scarps (Fig. 6). At the knick zones, the hillslopes are nearly vertical. Above the knick zones, the Grosse and Kleine Entle have incised up to 50 m into the moraine cover. In these areas, the channel floors of both rivers are approximately 10–15 m wide and reveal a braided pattern with longitudinal gravel bars that are several meters long. In the case of the Kleine Entle, the riversides are smooth and show meter-scale scarps.

The geomorphic features as outlined above can be interpreted as head ward shifting erosional fronts that have incised in response to base level fall after the retreat of the glaciers (see above and Schlunegger & Schneider 2005). In particular, the narrowing of the gorges towards the knick zones, the steepening of the riversides and exposure of bedrock on the channel floors imply ongoing incision. The scarps at the hillslopes bordering the channels were possibly formed by landsliding. Those processes are related to head ward incision and represent the lateral hillslope adjustment to the steeper channel gradient and to the greater channel depth after the passage of the headward shifting erosional front (Whipple et al. 1999).

At the knick zones, the occurrence of vertical hillslopes bordering the channel implies that, in these segments, the valley flanks are probably beyond the mechanical strength of failure. It also reflects that a response time is needed for hillslopes to adjust to a lowered channels floor. Above the knick zones, the presence of braided channels with longitudinal gravel bars implies sediment bypass. Furthermore, smooth hillslopes with scarps indicate the occurrence of hillslope creep processes.

Enduring incision of the Kleine Entle as documented by the geomorphometry possibly scales the process rates in the Rossloch-Bach watershed and those of the Schimbrig earth slide in particular. We will argue later that this will be the case when the knick-zone approaches the segment of the confluence between the Rossloch-Bach and the Kleine Entle.

4.2 Morphology of the earth slide and the Rossloch-Bach watershed

The Rossloch-Bach watershed and the Schimbrig landslide reveal three distinct domains of unconsolidated material (Fig. 8). They form the head and the toe of the earth slide, and the fan at the confluence with the Kleine Entle. The sedimentary fabric and the geomorphic properties of these domains are described below. In addition, attention will be focused on the identification of the nature of sediment transport and erosion in the Rossloch-Bach, because it represents the communication link between the landslide, the fan located at the confluence of the Rossloch-Bach with the Kleine Entle, and the Kleine Entle. Hence, any base level modifications will be transferred upstream to the landslide's head by this channel.

The head of the landslide is located at an elevation of 1420 meters above sea level beneath the concave debris fans of mount Schimbrig. There, the thickness of the sliding mass ranges between the decimeter- and the meter-scales. The vegetation cover is mostly intact, and scarps and crevices are generally absent. Only in the steepest portion, some decameter-scale slopes with scarps expose the regolith (Fig. 7F). These scarps were activated in the 1994 earth slide event and have been rejuvenated by the August 2005 storm event. At these localities, hillslopes dip at >20°.

Poorly consolidated accumulations of debris are abundant in the central part of the landslide, where outcrops reveal a minimal regolith thickness of 10 m. These accumulations are absent in the landslide's head. Laterally, the earth slide is bordered by ridges several meters to tens of meters high that strike in the down-slope direction. They are made up of Flysch bedrock covered by a decimeter-thick regolith cover.

At the toe of the slide mass, the debris is >15 m thick (Liniger & Kaufmann 1994a). In some locations, a thin layer of vegetation allows the sight of crevices in the loose and poorly consolidated sediment (Fig. 7A). In this area, the ridges made up of Flysch bedrock are several tens of meters high, and they strike perpendicular to the slip direction of the earth slide and hence to the general dip orientation of the topography. In particular, the rises with the huts of Schluck (local coord. 650347/199624) and Rossloch (local coord. 650039/199385) represent bedrock ridges that narrow the earth slide's path (Fig. 7B). In this whole area, the ground is wet with many puddles and partly covered with bog vegetation. Some decameter-high hills covered only with a decimeter-thick regolith cover and conifers on top show outcrops of Flysch bedrock (Fig. 7C). There, the bedrock is abraded and displays centimeter-long stria pointing in the down-slope direction (Fig. 7D). Those features were formed when the earth slide event exhumed the bedrock in 1994.

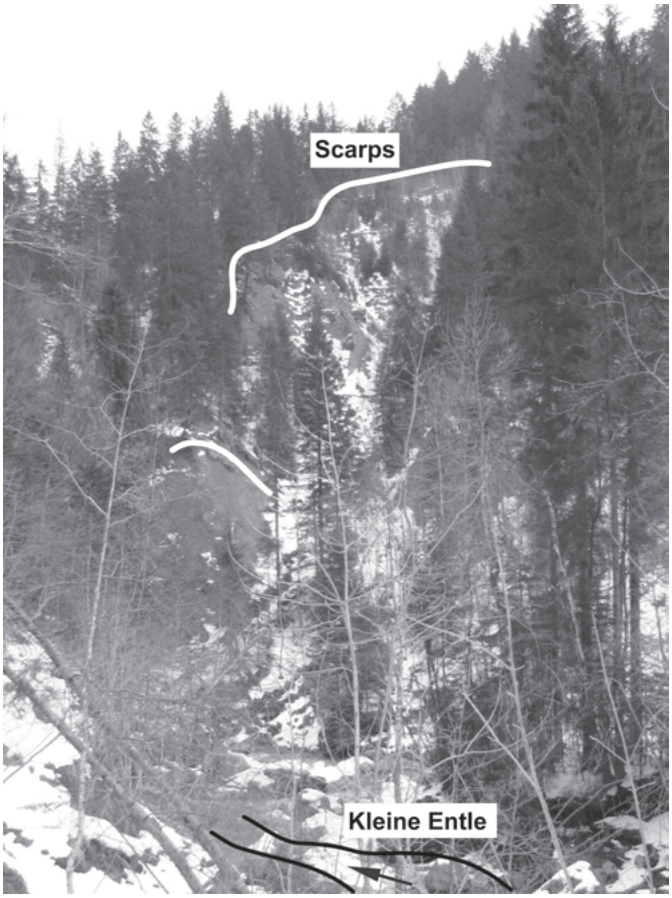

Fig. 6. Canyon of the Kleine Entle beneath the knick zone. Scarps indicate active hillslope processes. The exact location is presented on Figure 5.

The channel of the *Rossloch-Bach* is <3 m wide and generally enframed by decimeter-high levees. The channel floor has a block fabric, and in some locations the channel is blocked by loose accumulations of landslide debris. Downstream, the ridges of the Subalpine Molasse (Fig. 2) narrow the channel, forcing the riverbed of the Rossloch-Bach to flow in a straight path through this 200 m wide outlet. At the confluence with the Kleine Entle, the Rossloch-Bach flows across a short depositional fan, thereby meandering around accumulations of boulders and debris that are often present as meter-high rises with a centimeter-thick soil cover. This unit reveals a fan-shaped morphology with a cross-sectional width of 350 m. The fan deposits comprise multiple sequences of matrix-supported

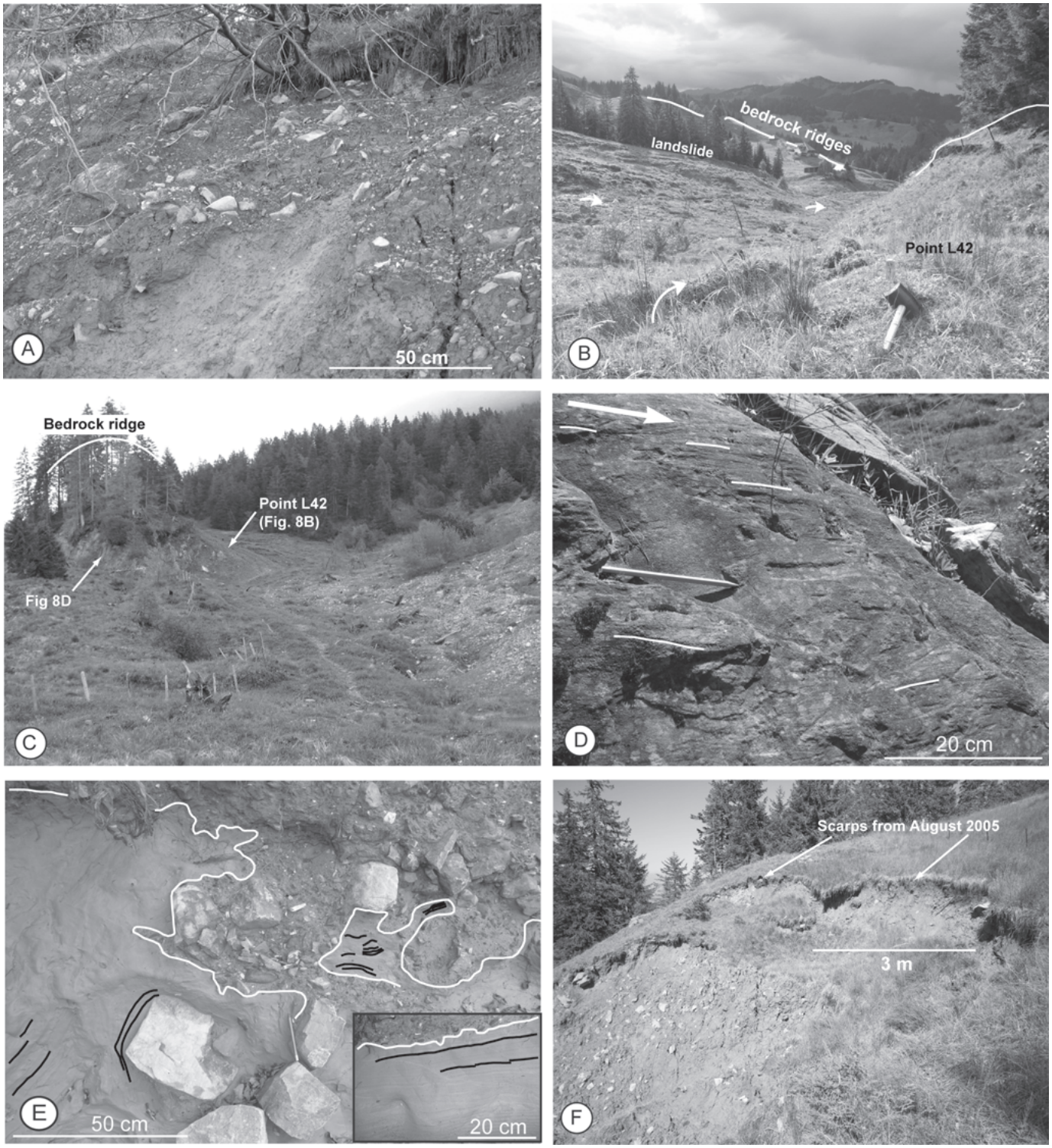

Fig. 7. Photos from the study area. The exact location is presented on Figure 8. A) poorly consolidated regolith with crevices and a thin vegetation cover at the toe of the landslide. B) View of the central part of the Schimbrig landslide with the huts of Rossloch, and the location of survey point L42 placed in the foreground. C) Flysch bedrock ridges in the central part of the landslide. D) Abraded bedrock with stria formed by the sliding masses. E) Diamicton embedded by laminated fine-grained sediments in the terminal fan at the confluence between the Rossloch Bach and the Kleine Entle. F) Scarps on the head of the landslide, triggered by the mid-August 2005 storm.

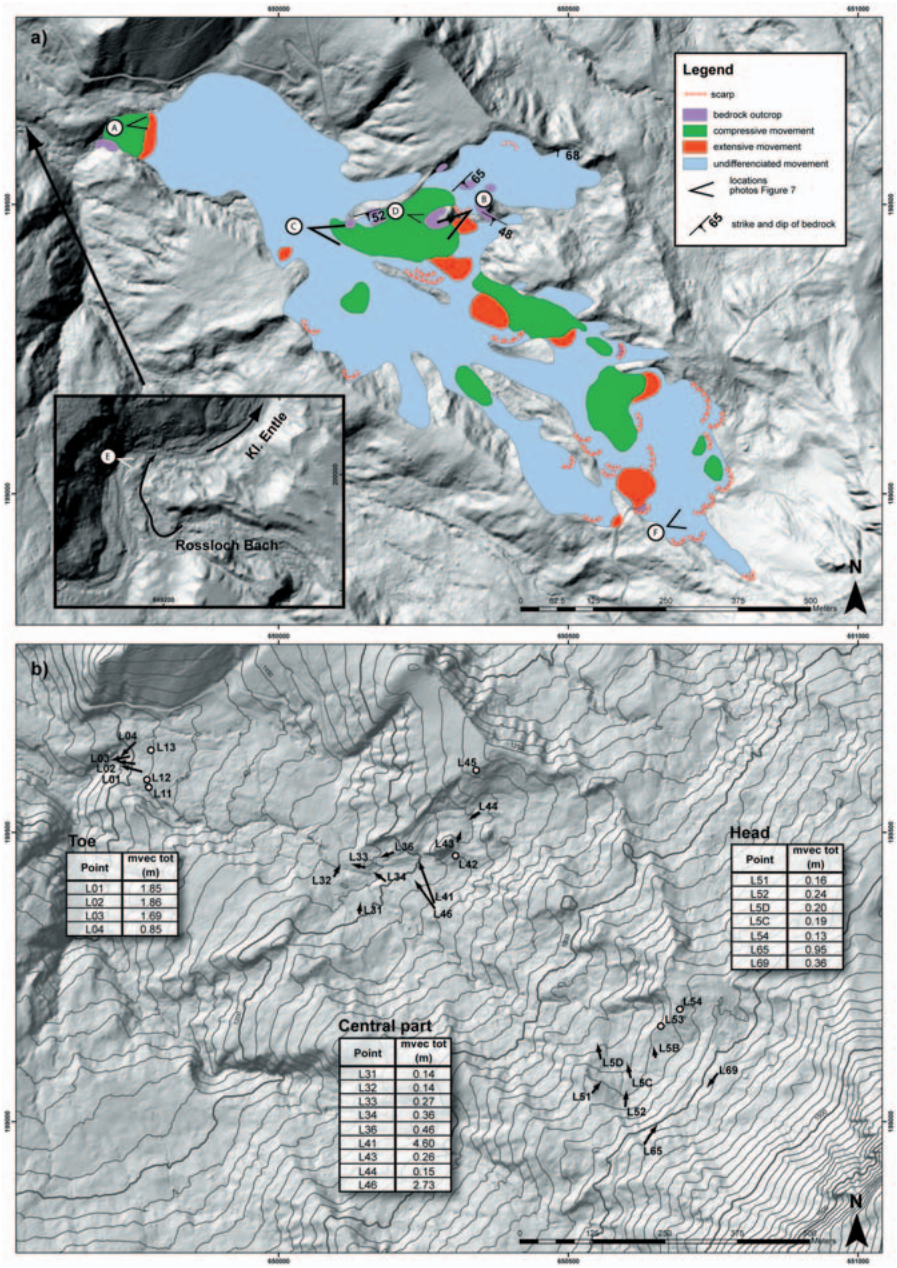

Fig. 8. a) Geomorphological map of the Schimbrig landslide with the extent of the 1994 earth slide event. Measurements of the strike of the bedrock show a nearly homogenous distribution. The bedrock forms the rises in the topography and narrows the landslide's path. Landforms like thrusts and transverse ridges showing concave upslope profile, as well as bulging zones that are mapped as compressive movements. Landforms like scarps and tension cracks (showing convex downslope profiles) are grouped under extensive movements.

b) Plots illustrating total displacements measured between 28th Sept 2004 and 15th November 2005. The arrows show the orientation of displacement. Note that the length of the arrows is indicative and not normalized. Refer to Table 1 for absolute movements. Points without arrow are below the quality threshold. Data© GIS Kanton Luzern, Coordinate system CH1903LV03, equidistance of contour lines 10m.

diamicton with angular clasts that have diameters up to 1 m wide. In some locations, parallel-laminated fine-grained sediments interfinger with these diamicton (Fig. 7E).

4.3 Survey

The results of the one year survey of the Schimbrig landslide reveal a spatial (Fig. 8) and a seasonal (Fig. 9) component in the pattern of slip rates. Note that Table 1 contains the results for the displacements measured between each survey and Figure 8b shows the total displacement during the whole period of survey.

A distinct seasonal trend is seen for almost all points. Specifically, highest slip rates were measured in late summer and autumn, whereas lowest slip rates occurred during the summer season. In addition, some locations reveal enhanced slip rates in spring. Figure 9a shows these trends in comparison with the climatic dataset. Interestingly, the heavy rainstorm event in August 2005 modified these trends differently along the slide mass. In particular, the points located on the toe (Line 0 in Fig. 9b) show an increase of slip rates during spring but no significant acceleration in response to the August 2005 storm. Note that the very low slip rates measured for Line 1 do not allow an unambiguous interpretation, but we can point out the expected

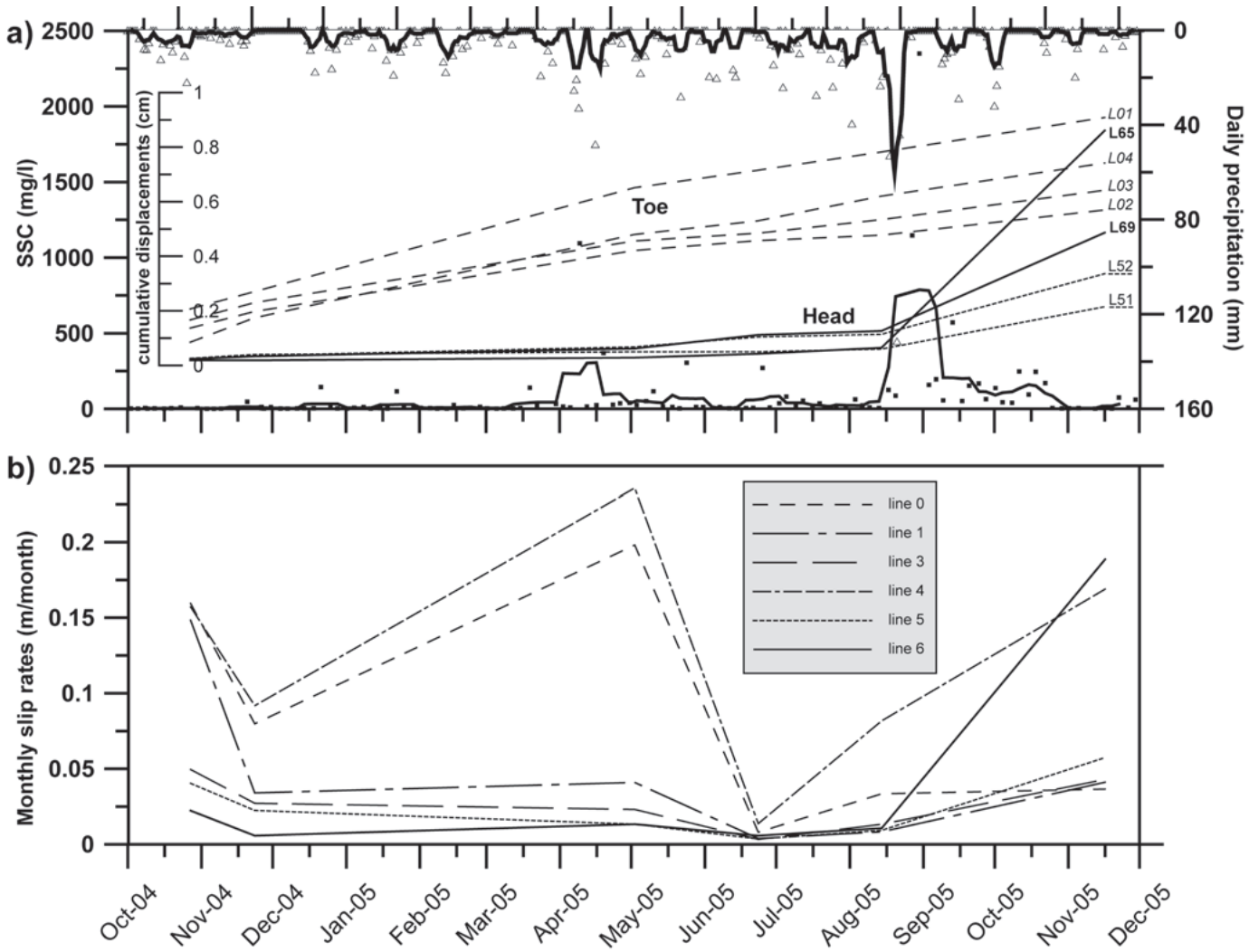

Fig. 9. a) Plot of the cumulative displacements of significant points on the toe and the head of the landslide compared to the SSC data (lower plot is a running average over 5 samples) and daily precipitation (upper plot is a running average over 5 samples).

b) Average monthly slip rates of the survey lines; e.g. line 0 is average of movement of points L01, L02, L03 and L04.

trend: constant slip rates in spring, very low or no movement in summer and increasing slip rates in autumn. Line 3, in the central part of the landslide, shows the same trend. Points on Line 4 experienced the highest slip rates over the year, but they do not seem to have been influenced by the August rainstorm. Indeed, the survey carried out in early August 2005 shows that slip rates started to increase before the rainstorm. On the head of the landslide, the influence of the rainstorm is more predominant. Lines 5 and 6 show significant increase in slip rates over the last survey period. In addition, the rainstorm in August had an impact on the landslide's appearance. In particular, decameter-scale earth flows and debris flows changed the local relief at the head of the landslide.

Similar to the seasonal variability, the results of the survey reveal a distinct spatial pattern in slip rates that varies between the head and the toe of the landslide (Fig. 9a). Specifically, the points at the head of the landslide show very little movement during the year, but were strongly affected by the August 2005 rainstorm. In contrast, the toe does not show a particular response to this event. In summary, the slip rates do not primarily depend on the slope angles of the topography, but it appears that there is a control of the earth slide's thickness on the seasonal trend of the measured slip rates.

5. Discussion and Interpretation

5.1 Mechanical properties of the earth slide

The data of the one-year survey imply that the Schimbrig earth slide has operated as a continuous process with rates that are controlled by the seasonality of climate, the thickness variations of the earth slide and the geometry of the underlying

bedrock interpreted from the ridges (bedrock outcrop on Figure 8a). A number of researchers have modeled rapidly-flowing landslides with non-Newton constitutive equations (Johnson 1970, Edgers & Karlsrud 1986, Savage et al. 1990). Here, we use a Bingham plastic model that best explains the observed spatial and temporal pattern of slip rates. In this model, deformation rates *(du/dt)* is a linear function of shear stress (τ) (Selby 1993; Allen 1997):

$$\tau = \tau_0 + \mu\left[\frac{du}{dt}\right] \quad (4)$$

where *(τ)* is the shear stress operating on the material, *(τ_0)* is the critical shear stress for material deformation and *(μ)* the viscosity. Equation (4) allows solving for the velocity *(u)* of a *(h)*-m thick Bingham plastic material:

$$u = \frac{1}{2\mu}\rho g h^2 \sin\alpha \quad (5)$$

where (ρ) is the density, *(g)* the gravitational constant, *(α)* the slope angle of the topography, and *(h)* the earth slide's thickness.

Equation (5) implies that variations in slip rates can be explained by a combination of thickness and climate variability and differences in dip angles of the earth slide. It also implies that any changes in the thickness of earth slides have a greater influence on slip rates than variations in hillslope steepness. Hence, this model explains why slip rates of the Schimbrig earth slide have been highest at the toe and the central part where the thickness of the material is substantially higher than at the head. This model also explains the seasonal variability in slip rates. In particular, late summer/autumn and early spring are the seasons with highest moisture contents in the soil (e.g., Schürch et al. 2006, for a similar situation). This is the case because snow melt in spring and decreasing temperatures in late summer/autumn result in a high retention of the pore water and thus in a low viscosity of the earth slide, which, in turns, promotes slip rates (see equation 5).

As described further above, the bedrock is present in several outcrops which implies the existence of a bedrock relief and a bedrock topography beneath the earth slide. It is possible that this preexisting topography was formed either during glacial periods or by combined channelized/hillslope processes during interglacial times. The geomorphic maps suggest that this bedrock morphology is partly responsible for the rerouting of the earth slide and thus for the pattern of slip directions. This is the case because bedrock ridges potentially form barriers for the sliding mass. In particular, as the path for the earth slide narrows, the material tends to accumulate above the narrowest part thereby experiencing compression.

In summary, the use of a Bingham plastic model allows us to propose two controls on the spatial variations in slip rates. These are (i) the down-slope increase of the earth slide's thickness that provides an explanation for the down-slope increase in slip rates, and (ii) the bedrock morphology that explains much of the slip direction variability at the lateral borders and at the locations where the earth slide's width decreases. In addition, the same model also allows interpreting the seasonal pattern of slip rates. In particular, the higher water content of the earth slide material in late summer/autumn and spring reduces the viscosity and thus promotes slip rates of the earth slide. Similar conclusions of continuous but seasonally variable landslide movements were also made by Coe et al. (2003).

Interestingly, the seasonal trend in slip rates was not uniformly influenced by the high-intensity rainfall in mid-August 2005. This implies that the mechanical properties of the material do not directly respond to an episodic pattern of rainfall. This interpretation is in line with the findings by Schürch et al. (2006) who found that variations in slip rates of the Erlenbach landslide (central Switzerland) is controlled by the seasonal variations in moisture content of the soil and not by the episodic character of rainfall events. These late-summer precipitation events, however, have a superimposed influence. They result in hillslope adjustment by local decameter-scale landslides and in initiation of debris flows (see below). The seasonal trend in the slip rates of the landslide body, however, is only locally disturbed during such events.

5.2 Debris flows

Debris flows are potentially responsible for the local re-distribution and export of sediment from the landslide to the channel network. They can be released in response to high-intensity rainfall events (Varnes 1978). Evidences for the consequences of such events are seen in the Rossloch-Bach watershed and on the Schimbrig earth slide. In particular, the matrix-supported diamicton that form a fan-shaped geometry at the confluence between the Rossloch-Bach and the Kleine Entle indicates the presence of a terminal fan constructed by debris flows. These flows potentially dam the Kleine Entle during events of high sediment discharge. We identified the diamicton as debris flow deposits sourced in the Rossloch-Bach watershed. The channel of the Kleine Entle was then dammed by the debris flow material, and the retained water formed a pond that resulted in the deposition of the laminated fine sediment. In support of the importance of debris flows for sediment transport from the landslide to the recieving Entle are observations in relation to the high-intensity precipitation event in August 2005.

5.3 Limits on process rates

The Kleine Entle watershed reveals two segments with different controls on rates of surface erosion and sediment flux. These two segments are separated by knick zones indicating that the Entle drainage is in the stage of head ward erosion and down-cutting. The adaptation of the Kleine Entle watershed to the lowered post-LGM base level is the driving force for erosion and sediment transport at and beneath the knick zones. In addition, exposure of bedrock at these particular locations reveals a supply-limited sediment flux. In the upper segment above the knick zone, however, processes are still

controlled by the higher base level of the LGM. There, the presence of gravel bars indicates a sediment bypass. As a consequence, the low channel gradient of the Kleine Entle above the knick zone and the limited transport capacity in this particular segment potentially also exerts a limit to the sediment flux in the Rossloch-Bach watershed. This stage of limit (or decoupling) will remain until the knick zone in the Kleine Entle reaches the confluence with the Rossloch-Bach. If this situation is established, enhanced incision will presumably enhance erosion in the Rossloch-Bach watershed and on the Schimbrig landslide, hence realizing coupling between the landslide and the trunk stream.

6. Conclusion

The Schimbrig earth slide shows a variety of topographic features, which reflect the presence of bedrock ridges at several locations. We supppose that the seasonality of climate and variations in the earth slide's thicknesses set the ultimate control for the magnitude and the pattern of slip rates. We propose that a Bingham plastic model for the Schimbrig earth slide explains much of how measured slip rates are linked to the observed topography, climatic variations and thickness variability. Interestingly, process rates in the Schimbrig region are still limited by the elevation of the LGM base level. At present, the watershed is in a stage of adjusting to the lowered post-glacial base level as indicated by knick zones in the trunk stream. At the time when these knick zones will reach the Schimbrig site, we anticipate a substantial increase in process rates and sediment flux in this region.

Acknowledgements

We thank Franz Schnyder (Geopoint Lütolf) for assistance in relocating old survey points. Gregor Stöckli and Thomas Heugel supported this research in the field and contributed to the successful survey. We are very grateful to Hanspeter Bärtschi for providing technical facilities in the field.

REFERENCES

Allen, P.A. 1997: Earth Surface Processes. Blackwell Science, Oxford. 404 pp.

Bieri, B. 1982: Geologie und Mineralwasser des Schimbriggebietes. Mitteilungen der Naturforschenden Gesellschaft Luzern 27, 41–95.

Caron, C., Lateltin, O. & Raetzo, H. 1996: Réactivation catastrophique du glissement de Falli Hölli (Préalpes fribourgeoise – Suisse). Quaternaire 7, 111–116.

Coe, J.A., Ellis, W.LO., Godt, J.W., Savage, W.Z., Savage, J.E., Michael, J.A., Kibler, J.D., Powers, P.S., Lidke, D.J. & Debray, S. 2003: Seasonal movement of the Slumgullion landslide determined from Global Positioning System surveys and field instrumentation, July 1998-March 2002. Engineering Geology 68, 67–101.

Cruden, D.M. & Varnes, D.J. 1996: Landslide Types and Processes. In: Turner A.K & Schuster R.L. (Eds): Landslides, Investigation and Mitigation, 257–277, National Research Council.

Edgers, L. & Karlsrud, K. 1986: Viscous analysis of submarine flows. Norwegian Geotechnical Institute, Publication 166, 1–9.

Gasser, U. 1966: Sedimentologische Untersuchungen in der äusseren Zone der subalpinen Molasse des Entlebuchs (Kt. Luzern). Eclogae Geologicae Helvetiae 59, 724–772.

Gasser, U. 1968: Die innere Zone der subalpinen Molasse des Entlebuchs (Kt. Luzern): Geologie und Sedimentologie. Eclogae Geologicae Helvetiae 61, 229–319.

Johnson, A.M. 1970: Physical processes in geology. San Fransisco, Freeman, Cooper & Co, 577 pp.

Kempf, O. & Pfiffner, O.A. 2004: Early Tertiary evolution of the North Alpine Foreland Basin of the Swiss Alps and adjoining areas. Basin Research 16, 549–567.

Korup, O. 2004: Landslide-induced river channel avulsions in mountain catchments of southwest New Zealand. Geomorphology 63, 57–80.

Korup, O. 2005: Large landslides and their effect on sediment flux in South Westland, New Zealand. Earth Surface Processes and Landforms 30, 305–323.

Lateltin, O., Beer, C., Raetzo, H. & Caron, C. 1997: Landslides in Flysch terranes of Switzerland: causal factors and climate change. Eclogae Geologicae Helvetiae 90, 401–406.

Liniger, M. & Kaufmann, B. 1994a: Rutschung Schimbrig, Geologisch-geomorphologisch-hydrologische Abklärungen und Sanierungsvorschläge. Geotest, Bericht Nr. L9434, 11 pp.

Liniger, M. & Kaufmann, B. 1994b: Rutschung Schimbrig, Ursachen, Entwicklung, Schadenszenario und Massnahmen. Geotest, Ergänzungsbericht Nr. L9434-B, 13 pp.

Matter, A. 1964: Sedimentologische Untersuchungen im östlichen Napfgebiet. Eclogae Geologicae Helvetiae 57, 315–429.

Mollet, H. 1921: Geologie der Schafmatt-Schimberg-Kette. Beitrag zur Geologischen Karte der Schweiz, N.F.37.

Pfiffner, O.A. 1986: Evolution of the north Alpine foreland basin in the Central Alps. Special Publication of the International Association of Sedimentologists 8, 219–228.

Raetzo, H., Keusen, H.R. & Oswald, D. 2000: Rutschgebiet Hohberg-Rohr (Plaffeien, FR) – Disposition und Aktivität, Bulletin für angewandte Geologie 5, 55–68.

Savage, W.Z., Amadei, B. & Cannon, S.H. 1990: Unsteady flow of Bingham viscoplastic material in an open channel. In: Proceedings of the National Colnference on Hydraulic Engineerings, July 30th –August 2nd, San Diego, California. American Society of Civil Engineering, 397–402.

Schlunegger, F., Burbank, D.W., Matter, A., Engesser, B. & Mödden, C. 1996: Magnetostratigraphic calibration of the Oligocene to Middle Miocene (30–15 Ma) mammal biozones and depositional sequences of the Swiss Molasse Basin. Eclogae Geologicae Helvetiae 89, 753–788.

Schlunegger, F., Jordan, T.E. & Klaper, E.M. 1997: Controls of erosional denudation in the orogen on foreland basin evolution: The Oligocene central Swiss Molasse Basin as an example. Tectonics, Vol. 16/5, 823–840.

Schlunegger, F., Slingerland, R. & Matter, A. 1998: Crustal thickening and crustal extension as controls on the evolution of the drainage network of the central Swiss Alps between 30 Ma and the present: constraints from the stratigraphy of the North Alpine Foreland Basin and the structural evolution of the Alps. Basin Research 10, 197–212.

Schlunegger, F. & Hinderer, M. 2003: Pleistocene/Holocene climate change, re-establishment of fluvial drainage network and increase in relief in the Swiss Alps. Terra Nova 15, 88–95.

Schlunegger, F. & Schneider, H. 2005: Relief-rejuvenation and topographic length scales in a fluvial drainage basin, Napf area, Central Switzerland. Geomorphology 69, 102–117.

Schürch, P., Densmore, A.L., McArdell, B.W. & Molnar, P. 2006: The influence of landsliding on sediment supply and channel change in a steep mountain catchment. Geomorphology 78(3–4), 222–235.

Selby, M.J. 1993: Hillslope materials and processes. Oxford University Press, Oxford. 451 pp.

Varnes, D.J. 1978: Slope movement types and processes. In: Schuster, R.L. & Kriezek, R.J. (Eds): Landslides – Analysis and Control. National Academy of Sciences Transportation Research Board, 12–33.

Whipple, K.X., Kirby, E. & Brocklehurst, S.H., 1999: Geomorphic limits to climate-induced increases in topographic relief. Nature 401, 39–43.

Manuscript received July 14, 2006
Revision accepted December 14, 2006
Published Online First July 20, 2007